Compliant variable negative to zero to positive stiffness twisting elements

Amoozandeh Nobaveh, Ali; Herder, Just L.; Radaelli, Giuseppe

DOI
10.1016/j.mechmachtheory.2024.105607

Publication date
2024

Document Version
Final published version

Published in
Mechanism and Machine Theory

Mechanism and Machine Theory 196 (2024) 105607

Contents lists available at ScienceDirect

Mechanism and Machine Theory

journal homepage: www.elsevier.com/locate/mechmt

Research paper

Compliant variable negative to zero to positive stiffness twisting elements

Ali Amoozandeh Nobaveh *, Just L. Herder, Giuseppe Radaelli

Precision and Microsystems Engineering Department, Delft University of Technology, 2628CD, Delft, The Netherlands

ARTICLE INFO

Keywords:
Compliant mechanisms
Variable stiffness
Zero stiffness
Negative stiffness
Twisting beams
Bistable mechanisms

ABSTRACT

Compliant mechanisms have the potential to be utilized in numerous applications where the use of conventional mechanisms is unfeasible. These mechanisms have inherent stiffness in their range of motion as they gain their mobility from elastic deformations of elements. In most systems, however, complete control over the elasticity is desired. Therefore, compliant mechanisms with variable, including zero, stiffness can have a great advantage. We present a novel concept based on the prestressing of open thin-walled multi-symmetric beams. It is demonstrated that by changing the prestress on the center-axis of these beams, a range of variable torsional stiffness can be achieved. For beams with a large warping constant, the stiffness changes from positive to zero and negative as the prestress increases, while for beams with a near-zero warping constant, the range of neutrally stable twisting motion increases. A planar equivalent is shown in this work to elucidate the notion, and numerical and experimental analyses are performed to validate the prestress-related behavior.

1. Introduction

Compliant Mechanisms (CM) have been developed by researchers to make more efficient mechanical devices that can work in specific conditions such as vacuum or high temperature [1]. These mechanisms can integrate several functionalities into one system, leading to lighter and more space-efficient designs. Moreover, due to their monolithic design, these mechanisms are potentially suited for applications where minimized friction, backlash, and particle generation are important, as well as for applications where, due to the small sizes, assembly is not viable. CMs are widely being applied to precision devices and even some daily-used products. Aside from that, there are ongoing investigations into how to transfer the principles of compliant mechanism design to other research fields, such as soft robotics [2,3], wearable robotics [4–6] Micro Electronic Mechanical Systems (MEMS) [7], morphing structures [8–10], origami [11], and metamaterials [12]. There are several studies on the design of compliant units that are useful for incorporation into modular architectures. Examples include linear motion guides [13], constant force generators [14] and prescribed kinetostatic behavior generators [15–17], bistable units [18,19], twisting elements or revolute joints [20,21].

CMs derive their mobility from the elastic deformation of their elements, which means that normally they have an inherent positive stiffness in their range of motion. Therefore, to actuate a CM, a certain amount of energy should be added to the system, which is stored in the material in the form of elastic strain energy. Once the compliant mechanism is not actuated, this energy will be released to bring the mechanism back to its natural, undeformed configuration. This integration of motion and energy storage into one element is beneficial for several applications. However, in some applications, providing this energy to move the mechanism in its intended range of motion is not desirable because the system requires more power for each cycle and the overall efficiency decreases.

* Corresponding author.
E-mail address: a.amoozandehnobaveh@tudelft.nl (A. Amoozandeh Nobaveh).

https://doi.org/10.1016/j.mechmachtheory.2024.105607
Received 28 August 2023; Received in revised form 14 December 2023; Accepted 31 January 2024
Available online 7 March 2024

This means that in these applications a range of constant potential energy, or in other words, a range of neutral stability would be convenient. There are several ways to achieve a range of elastic neutral stability, e.g., utilizing anisotropic materials [22–24], prestressing the structure either by imposing a constraint [25], or by plastic deformation [26–28], or by introduction of a movable deformed region [29,30].

In some applications of CM, one or more element(s) have specific functionality, and it is not feasible to remove them and their inherent positive stiffness. In these cases, it is not possible to change the whole design to make the mechanism neutrally stable with one of the above-mentioned methods. Therefore, to achieve neutral stability in these cases, a common way is to compensate the inherent positive stiffness of the system with the exact same negative stiffness from another system to achieve a range of zero stiffness. Using the negative stiffness to compensate for positive stiffness is widely researched in the literature [31,32], both for linear negative stiffness [33] and nonlinear negative stiffness compensators [34]. In addition, there are numerous applications in the literature that require variable stiffness on demand, which means the part with negative stiffness should be able to change its amount so that the overall stiffness of the system becomes tunable [35]. These applications are ranging from aerospace engineering [36–38], to medical devices [39,40], wearable devices [41–43], and vibration control [44]. In all these applications, the shared desired characteristic of having variable stiffness allows them to alter the overall system behavior in a specified direction on demand.

However, looking at these variable stiffness concepts, they are mainly developed for translation motion. There are a few instances of concepts with a variable rotational stiffness, like the one shown by Zhao [45] or the one shown by Smreczak [46], which are both based on straight planar flexures that lose their stiffness trough column buckling. There are also a handful of concepts that exhibit zero or negative stiffness, which have the potential to be developed into variable stiffness systems. Bilancia et al. [47] demonstrated a zero torque compliant rotational joint that uses prebuckled beams to achieve negative stiffness to compensate for the mechanism's positive stiffness. Li et al. [48] presented a torsional negative stiffness mechanism utilizing several thin strips. Schultz [49] presented an airfoil-like bistable twisting element that was made from two precurved shells connected to each other. Seffen and Guest [50] further researched similar effects, and later, Lachenal et al. [51] presented a bistable twisting I-beam where the precurved flanges assembled on the beam's web to provide a negative stiffness twisting behavior.

In this work, we are introducing two concepts for twisting compliant elements. The first concept can provide variable torsional stiffness from negative to zero to positive. The second concept can provide on-off switchable torsional stiffness, which changes the element's inherent positive stiffness to zero stiffness. Both concepts works based on the fact that as the center axis of a multi-symmetric thin-walled beam shortens, the outer parts of the beam's section go under compression. As compression is the stiffest mode of deformation and requires high elastic energy, the outer parts start to deform in other forms instead, in order to facilitate the web shortening with a lower overall elastic energy. In one concept where the beam has flanges and a high warping constant, after the shortening, the beam twists to facilitate the shortening with lower amount of energy. This twist can happen in both directions and therefore, it is bistable. By changing the amount of shortening, the mechanism's stiffness varies from its inherent positive to zero and more negative stiffness. In the other concept, the flanges of the beam are removed. Therefore, the outer parts of the webs start to buckle under the compression due to the center axis shortening. This locally buckled part of the webs can move along the structure upon twisting the beam without requiring extra energy, and provides a range of neutral stability. Therefore, the mechanism's stiffness switches from the inherent positive to zero upon buckling due to the axial shortening. In this case, by increasing the preload, the range of motion with zero torsional stiffness increases. These two designs and their effective parameters are explored and modeled with FEM and experiments. Moreover, a simplified planar equivalent is presented that helps with understanding the principles behind the concepts.

The paper is structured as follows: In Section 2, an overview of the concept and its principle of working is introduced. Also, a planar equivalent model is introduced for a better understanding of the beams' behavior. The definition of effective parameters, together with the finite element solver and the context of experimental verification procedures, are elaborated in Section 3. In Section 4 the resulting behavior from the two designs with different preloads are shown. A discussion on the results and possible improvements are given in Section 5, and the conclusion beside possible applications of these concepts are given in Section 6.

2. Concept overview

The geometry of the concepts is shown in Fig. 1. Both concepts are long, thin-walled extruded beams with transverse slits running the length of their multi-symmetric webs. These slits allow for shortening of the center axis, implying longitudinal preload. The First concept Fig. 1(a), also has flanges to enable warping along the structure and the second concept Fig. 1(b) is only made form the multi-symmetric webs. A center hole is made in both concepts, which makes room for an element, i.e., wire, for preloading and shortening of the beams.

The working principle of both beams to achieve neutral and negative stiffness under prestress can be clarified by understanding their total energy states in their twisting range of motion. This energy is depicted in Fig. 1(a) for the beam with flanges. Two minima can be seen in the range of motion. There is also a peak in between these two minima or stable states. This peak indicates that the beam is not stable between these two and hence exhibits a negative stiffness. Fig. 1(b), also shows two minima for the beam without flanges; however, it has a flat energy state in between these two minima. This flat section indicates that for a relatively large range between its stable states, the beam exhibits neutrally stable twisting motion, i.e., zero torsional stiffness.

Different techniques could be used to contract the web(s) and prestress the mechanism with a displacement to achieve these behaviors. Here, we employed transverse slits along the web(s) such that a longitudinal displacement along the axis of the beam's center could make the beam shorter with less reaction force. These slits and the displacement Δd that causes the longitudinal prestress are shown in Fig. 1.

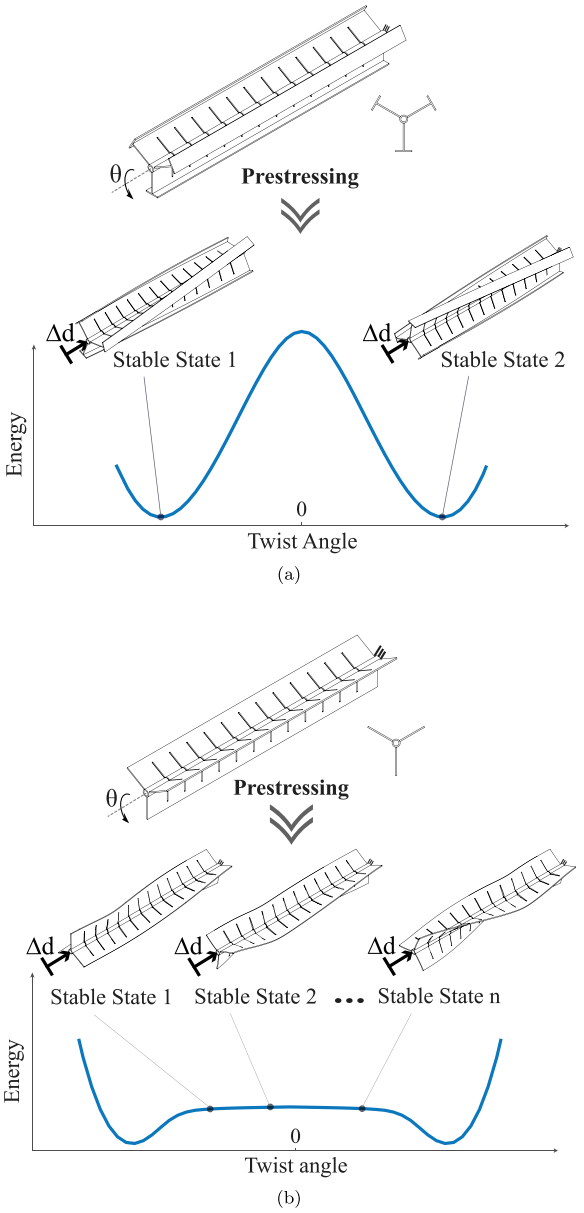

Fig. 1. The geometry of the multi-symmetric beams and their transverse slits are shown together with the qualitative energy – angle graphs of them. The prestressed beams exhibit two stable twisted forms. (a) The beam with flange (high warping constant) possesses an energy peak between the two minima and, therefore, bistable behavior. (b) The beam without flange (near-zero warping constant) exhibits a flat energy state and, therefore, neutrally stable behavior between the two minima.

We also propose another way of understanding the principle of the presented design using a simplified planar equivalent, Fig. 2. To make this planar representation of the beams, we used a set of parallelograms, where the deviation in edge angles of each parallelogram from 90° represents the twist in each section of the beam. Therefore, in this model, when the beam is unstressed, all parallelograms are straight. To represent different stiffnesses of the beam sections in the planar equivalent, two torsion springs were added to each parallelogram. One is between two perpendicular links of each parallelogram (red springs), which keeps the parallelogram in its initial rectangular shape. These springs represent the torsional rigidity of the beam's sections. By increasing this rigidity, it is harder to twist the beam, which, in its planar equivalent, means that it is harder to make each parallelogram deviate from their initial rectangular shape. The second spring is positioned between the vertical links of two adjacent parallelograms (blue springs). These springs maintain the angles of adjacent parallelograms and reflect the ability to transfer twist to the following section of the beam. By increasing this rigidity, it becomes more difficult to make a sharp transition in the twist angle from one element to its neighbors. In planar equivalent, it becomes more difficult to make each parallelogram diverge from the angle of its neighbors.

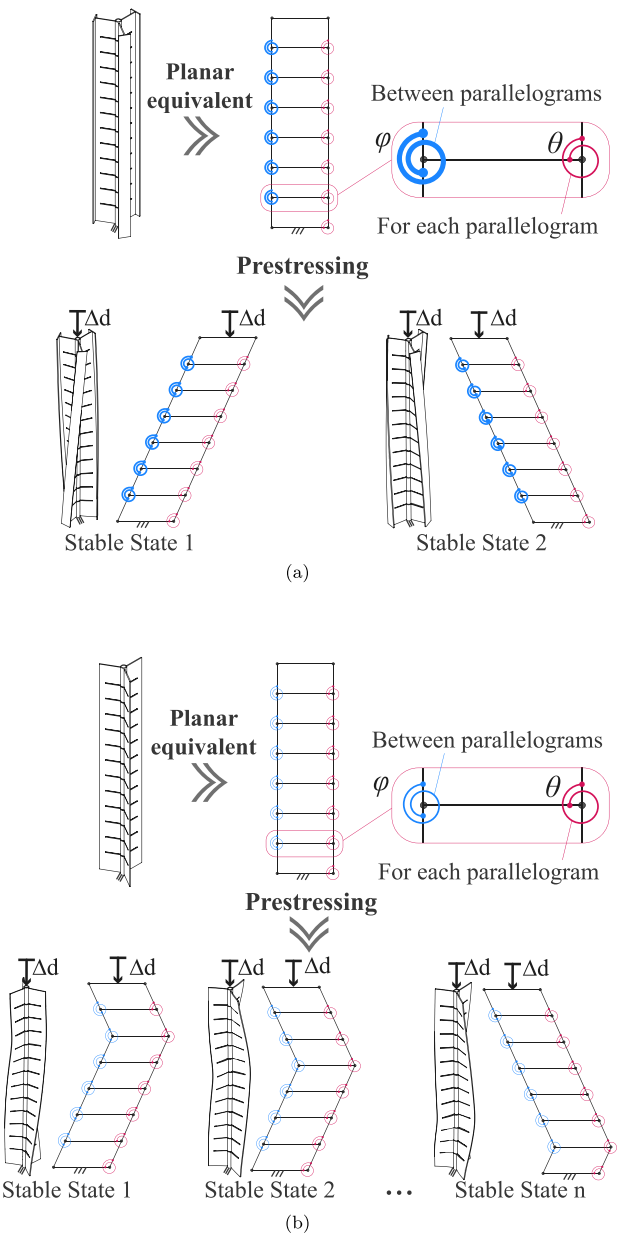

Fig. 2. The planar equivalent of the beams with the red springs representing the torsional constant, and the blue springs representing the warping constant. (a) The beam with flanges has a high warping constant and, as a result, exhibits uniform twist. (b) The beam without flanges has a near-zero warping constant which alows for transition of bent location along its length, and maintains a constant total energy based on Eq. (1). (For interpretation of the references to color in this figure legend, the reader is referred to the web version of this article.)

This spring stiffness can be related to the beam section's warping constant. In prior research, we have shown that the warping of an evenly extruded beam is the primary cause of twist transfer along its length [52]. In Fig. 2(a, b), the torsional rigidity of both beams is on the same order of magnitude; hence, the red springs are depicted as being sized comparably. However, the beam with flange has a warping constant that is an order of magnitude more than the beam without flange. Therefore, the blue springs on beam (a) are considerably more rigid, depicted as being thicker.

Under a vertical displacement Δd, the energy stored in the planar equivalent is the sum of all the energies stored in springs:

$$U_{\text{total}} = \frac{1}{2}\sum_{i=1}^{n}(k_{\text{red}_i}\Delta\theta_i^2 + k_{\text{blue}_i}\Delta\varphi_i^2). \tag{1}$$

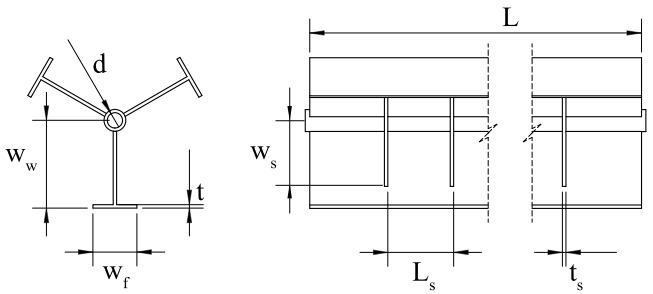

Fig. 3. The design parameters of the beams.

In the beam with flanges, the stiffness of the blue springs is significantly greater than that of the red springs; consequently, the majority of deformation occurs in the red springs when the structure is prestressed to reduce the overall energy. This will result in the uniform bending to the right or left, i.e., equivalent to a uniform CW or CCW twist angle for the beam. Now, if we attempt to shift the upper section of the structure horizontally, i.e., similar to twisting the free side of the beam, it will snap into the stable position on the other side, i.e., equivalent to torsional bistability.

In a similar manner, the beam without flanges initially displays a uniform bend to one side; but, upon horizontal displacement of the top portion to the opposite side, one of the parallelograms snaps to its inverted stable condition, since it is much less dependent on the angle of its neighboring parallelograms. As this horizontal displacement of the top portion continues, the number of inverted parallelograms increases and the point where the tilt angle inverses descends from the top to the bottom. Based on Eq. (1), the transition between these states requires no additional energy. Therefore, horizontally shifting the top portion of the structure (similar to twisting the beam between its stable states) goes without change in energy and is therefore neutrally stable. In the actual beam without a flange, the bent portion of the webs can move along the structure without consuming energy and provides a range of zero torsional stiffness.

3. Methods

In the following subsections, the effective design parameters of the concept are elaborated. A Finite Element Model (FEM) to analyze the beams' behavior in different preloading conditions is presented, followed by an explanation of the experimental setup for verifying the results.

3.1. Design parameters

The current design's main principle is based on shortening the center axis of a thin-walled multi-symmetric beam to achieve neutral- or bi- stability. It will be shown that the amount of shortening improves the captured behavior. Therefore, this parameter is subject to investigation. However, the design of the web and its dimensions are remaining fixed throughout all results. Therefore, here we discuss the reasoning behind the selection of this shape and its design parameters.

There are several ways to decrease the compression stiffness of the center axis of the beam in order to achieve local shortening by implying less stress to the structure, i.e., using non-homogeneous material where the middle part is softer than outer part, or thickening the webs towards the outside, or making several slits in the center part of the sections throughout the beam, which is the solution that is used in this work. These slits help the structure to significantly reduce the longitudinal stiffness along the center axis with respect to the outer parts to allow for shortening. The size and number of these slits (n) are selected based on preliminary investigation and they are kept the same for all the simulations and prototypes. The effect of using insufficient number of slits is later explained in Section 5. Other design parameters are all indicated in Fig. 3. These parameters are arbitrarily selected and can be tuned for different applications and from preliminary investigation they appear to have only a minor contribution to the overall concept. The web width (w_w) is 20 mm, the flange width (w_f) is 15 mm for the beam with flange, the axial hole diameter (d) is 3.5 mm, the thickness (t) is 0.9 mm all over the beams, the length of the beam (L) is 200 mm, the slit width (w_s) is 15 mm, the slit thickness (t_s) is 0.5 mm and the length of each section (L_s) is 10 mm, with (n = 19) slits along the beams.

The geometry, loading, and constraints are all axisymmetric; therefore, it is possible to reduce the model to only a one-web structure with axisymmetric constraints, as shown in Fig. 4. This reduces the computational cost, and to match reality, everything will be multiplied by the number of webs (m). It is important to mention that for spatial stability in a physical prototype, the number of webs in one beam should not be less than three ($m \geq 3$), so that all forces caused by the shortening and bending of each web can be supported by the two other webs and the structure remains stable. This means that not only three, but any number of multi-symmetric webs larger than three will work for this structure, as shown in Fig. 4.

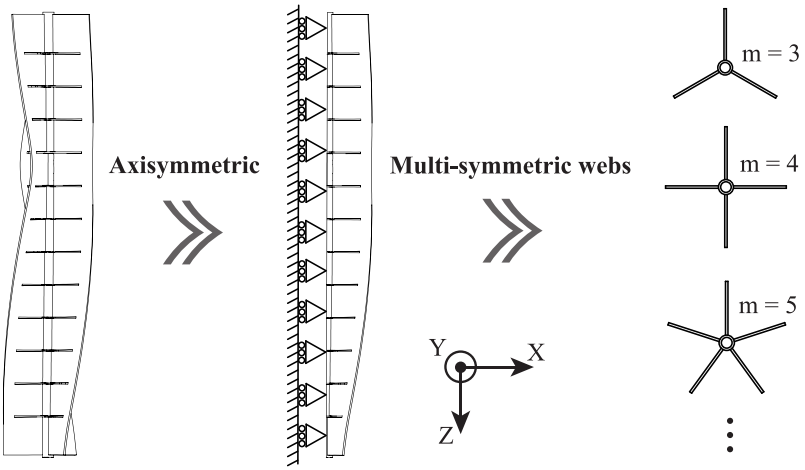

Fig. 4. The axisymmetric constraint simplifies the multi-symmetric beam to a single web. The number of webs (m) on beams must be at least three for spatial stability.

3.2. FEM

For both set of simulations, only one web from each beam is modeled with axisymmetry constraints similar to Fig. 4 as discussed in Section 3.1. The beams' web is constrained in all translations at the axis-point of the grounded side as shown in Fig. 5 and constrained in X and Y translational directions at the axis-point of the prestressed (actuated) side. To constraint the rotation on the grounded side of the beam a Y translational constraint applied to the middle point of the web. In addition, a Z rotation match between the axis-point of the actuated side and the middle point of the actuated side was added.

The simulation includes two steps. First, a longitudinal displacement (Δd) is applied to the axis-point of actuated side of the beams; simultaneously, a rotation (RotZ) is applied to assist its transitioning to a twisted state. The twist angle at the end of the preloading step was registered as θ. In the second step, a twist angle in the other direction with twice the size of the initial registered angle, i.e., -2θ, was applied to the beam and the reaction moment in the axis-point of actuated side is registered to form the moment – angle graphs of the beams.

For the simulations, the eight-node shell element, shell 281, from ANSYS Parametric Design Language (APDL) is selected as the constructing element. The material properties are set to be similar to the prototypes material, Nylon (PA12), with Young's modulus of 1.7 GPa and Poisson's ratio of 0.38. A nonlinear solver was used, with minimum 40 steps for preloading depending on the (Δd) and minimum 50 steps for capturing the moment – angle behavior depending on the range of rotation.

3.3. Experimental setup

Two sets of beam with and without flanges are fabricated using multi-jet fusion additive manufacturing method with Nylon (PA12) as the material, as shown in Fig. 6(a).

The beams are initially prestressed by providing displacement using an M2 threaded rod within the beams' center axis. This displacements range from 0 to 4 mm with increments of 1.0 ± 0.06 mm for the beams without flange, and 0 to 2.8 mm with increments of 0.7 ± 0.06 mm for the beams with flange. With each degree of prestress, the moment – angle of the beams was measured using a universal test machine, Zwick Z005, with a separate torque meter module, HBM T20WN as shown in Fig. 6(b).

Similar to the constraints that are implied in the FEM, each of the prestressed beams is clamped on one side to the measuring point of the machine, and on the other side, a rotation is progressively applied to the actuated side of the webs.

4. Results

Fig. 7 shows the moment – angle graphs of both with and without flange beams. They share the same web dimensions (see Fig. 3) and the same number of slits (n = 19). The longitudinal preloading in their center axis increases in four steps, as discussed in Section 3. Fig. 7(a,c) are for the beam without flanges from numerical model and experiments respectively. It can be clearly seen that the beam has its inherent positive stiffness when no prestress is applied, and upon applying prestress, an increasing range of zero moments and neutrally stable behavior are achieved. Fig. 7(b, d) show the numerical model and experiment results for the beam with flanges. These results show that this beam also shows its linear inherent stiffness without preload, and upon 0.7 mm preload it shows a short range of near-zero stiffness. Finally, a clear bistable behavior, negative torsional stiffness, can be seen upon 1.4 to 2.8 mm of preload.

It is important to note that the beams that are used in experiments have four webs; therefore, to make the results comparable with the single web with axisymmetric constraint from FEM, the resulting moments from experiments are divided by four, and all the results are for a single web (beam without flange) or a single web and flange (beam with flange).

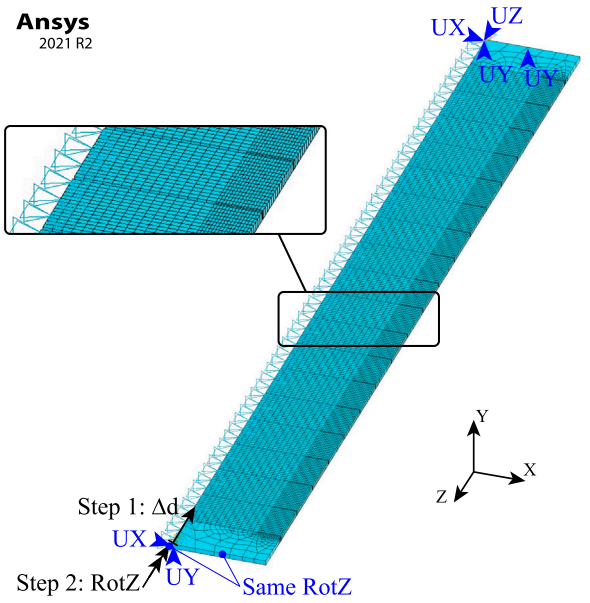

Fig. 5. The constraints on the fixed and actuated sides of the web are shown. An axisymmetric constraint is applied similar to what is shown in Fig. 4 along the web.

(a) (b)

Fig. 6. (a) The prototypes were made from nylon (PA12) using multi-jet fusion 3D printing and prestressed using threaded rods. (b) The measurement setup shows the actuating and reaction moment measuring sides of the preloaded beam that is clamped to the machine.

5. Discussion

It is demonstrated that the prestressing of the center axis of an open, thin-walled, multi-symmetric beam can have significant influence on its torsional stiffness. Both the with- and without-flange beams exhibit two local minima at the ends of their range of motion following prestressing. The beam with flanges displays an energy peak between these two minima, indicating bistable behavior, Fig. 7(b) and (d). The beam without flange exhibits a flat energy between the two minima, indicating a neutrally stable

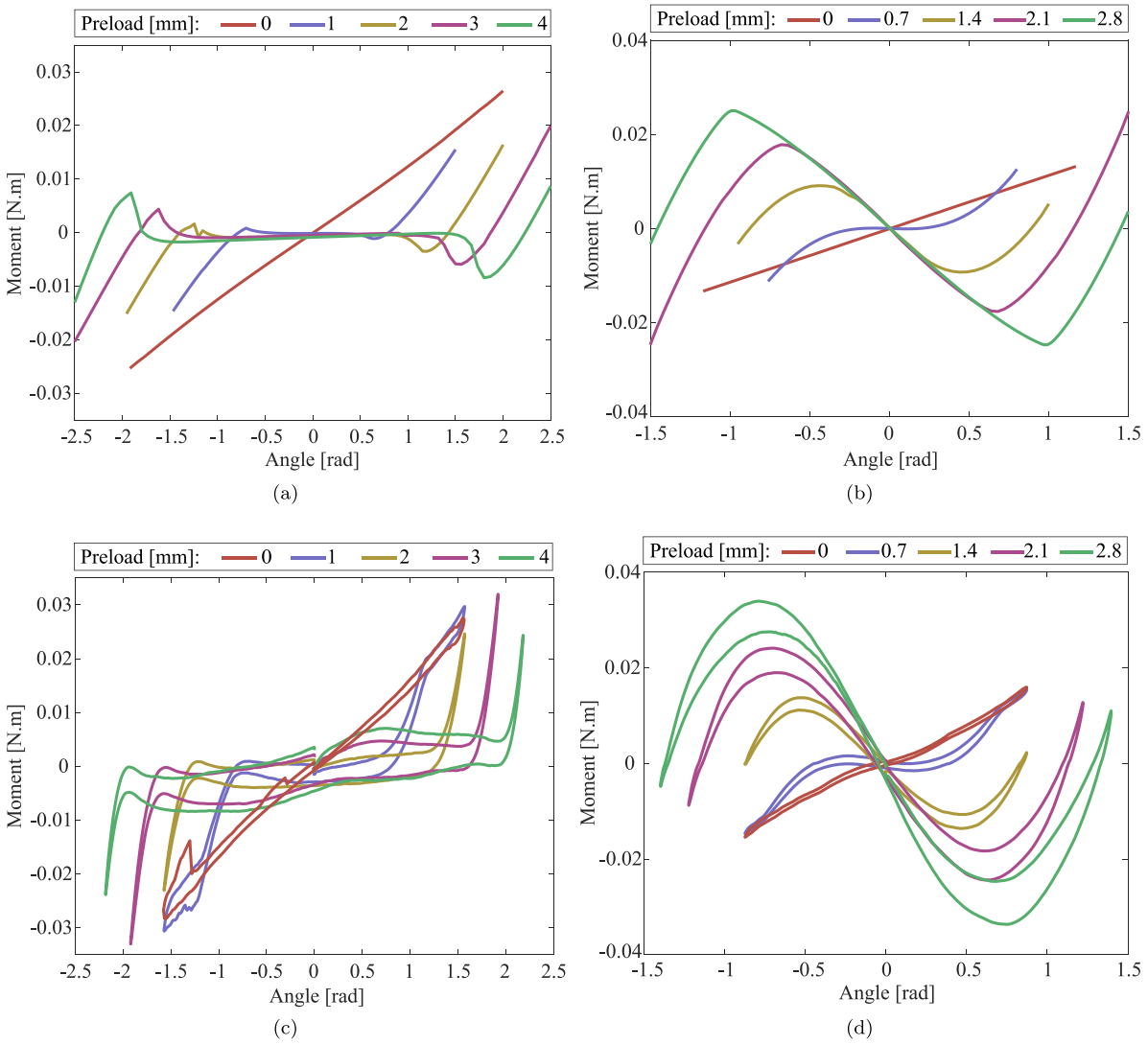

Fig. 7. The moment – angle graphs of the beams upon different preloadings. (a) and (c) show the numerical and experimental results for the beam without flange under axial preloads Δd of 0 to 4 mm. (b) and (d) show the numerical and experimental results for the beam with a flange under axial preloads Δd of 0 to 2.8 mm. (For interpretation of the references to color in this figure legend, the reader is referred to the web version of this article.)

behavior, Fig. 7(a) and (c). In addition, it is demonstrated that both bistable behavior and neutral-stability range can be enhanced by increasing the beams' prestress. Consequently, the presented concept can provide a twisting element with variable stiffness that can achieve negative, zero, and positive torsional stiffness for beams with high warping constant, and a positive and tunable range of zero torsional stiffness for beams with near-zero warping constant.

A rather large range of zero torsional stiffness motion for the compliant beam without flange and a high bistable energy storage in beam with flange were obtained by the parameters that are used in this work to demonstrate the functionality of the concept. These behaviors can be further enhanced to maximize design functionality based on specific requirements of certain applications of these concepts.

The investigations in this paper show a clear trend between the amount of prestress and the resulting behaviors of the beams, i.e., peak moment in bistability and range of neutral stability. The exact relation between prestress and the achieved behavior can be further investigated in future research.

Some design parameters, such as the number of slits, have effects on the overall functionality of the presented concept and should be carefully selected. In Fig. 8 we have shown that increasing this number will cause a smoother behavior for the twisting element, and avoid multi-stability due to the snapping of bistable units (parallelograms) along the beams. However, after selecting a sufficient amount of slits, this effect vanishes and no further investigation is required for it, therefore, it is also excluded from the results of the current work.

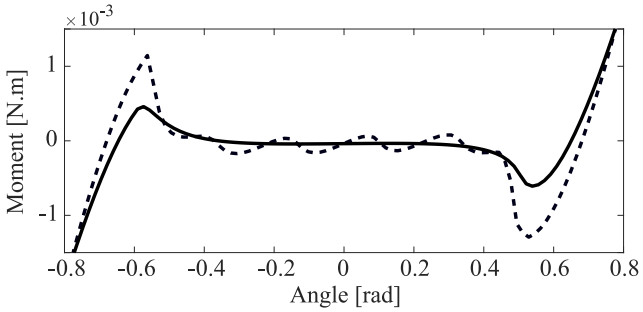

Fig. 8. The effect of using an insufficient number of slits (n = 7) is shown with a dashed line, and the sufficient number of slits for prototypes and simulations (n = 19) is shown with a solid line. All other parameters are similar to those described in Fig. 3, and only the number of slits is changed. The results are from the simulation with the same constraints as Fig. 5.

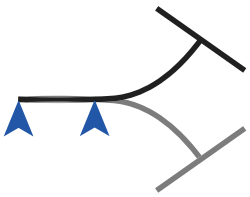

Fig. 9. Bistable beam's sectional deformation changes from black to gray upon higher changes in reaction moments.

The experiments and simulations show very similar results and trends, which indicates the validity of the results. There are small discrepancies that can be due to different effects. To begin with, there are geometrical differences between the model and the prototype: in the prototype, a hole in the center was added for prestressing the beams; additionally, small fillets were added between webs and flanges in the actual prototypes to ensure a good connection. The thickness of the prototypes also deviates ±0.05 mm from the model, which can cause differences in the results. Secondly, idealized constraints are applied to the model; however, in experiments, making these constraints exactly like what we proposed in the simulations is not a viable option. There are a few details that are different in the constraints of the model with respect to the experiments. Firstly, in the simulation the prestress is applied exactly in the center axis of the beam. However, it is not feasible in the experiment. Therefore, in the experiment the prestress is applied to the geometry onto a circular thickening with 10 mm diameter, which is part of the printed geometry, see Fig. 6(a). Also, there is a difference in the way the rotation is applied to the web in simulation with respect to the experiment. In the experiment, namely, a cross-shaped clamp holds the webs until about half of their lengths. In the simulation, on the other hand, there is only a rotation constraint at a location halfway the length of the web. This makes that the way the webs can deform in the cross-sectional plane is different. At high levels of preload, a sudden change in cross-sectional shape was observed. This change in shape is illustrated in Fig. 9. This explains the sharper changes in the reaction moment of the simulation results for larger preloads, see Fig. 7(b). In simulations with lower prestress, preloads 0.7 mm (purple) and 1.4 mm (yellow). This behavior is not strong. Therefore, smoother changes between positive and negative stiffness were achieved for the bistable beam. Similarly in Fig. 7(a), for neutrally stable beam a smoother change to a flat part was achieved in the experiments comparing to the simulations, since the clamping imperfections gave room for webs to have some deformations during rotation, preloads 1 mm (purple) and 2 mm (yellow).

Another observation is the minor asymmetry in the change phase between stiff mode and zero stiffness mode in simulations. This happened due to the hard convergence and not having sufficient steps during this switch. One can ask then why more steps were not utilized, and the answer is that we used them. However, we could not achieve convergence at all since zero-stiffness structures are very hard to control and converge, and the number of steps and controlled nodes should have a close match for convergence.

Another difference can be seen in the stiffness of the beams outside the range of zero or negative stiffness. This is also because of the differences in constraints; in FEM, the movement of the beam in the longitudinal direction (Z) is free, but in experiments, the side clamps also partially limit this movement. This makes the structure stiffer in torsion because the twist is coupled with a shortening in the longitudinal direction. Also, in FEM, the preloading displacement limits the longitudinal movement of the beam's axis in both directions. In experiments, however, it is only done by shortening the axis line with a screw, which only limits movement in one direction. This means that after a certain amount of twist, the beams become short enough to effectively release the preload. This effect is clearly visible in Fig. 7(c,d) where the purple line matches the linear red line after a certain amount of twist. Another important observation is that, a rather large hysteresis loop in experiments is captured. This effect is mainly due to the use of nylon

as the prototype's material, and this loss of energy due to the internal friction increases as more preload is added to the material. This internal friction can also help in the case of neutrally stable beam to keep it in certain stable positions and avoid imperfections to always bring this beam to a specific deformed state. These imperfection in the experiments can cause a preferred inflection point in the prototypes. However, by having more consistent geometry, the beam can have multiple points of inflection. Lastly, some small imperfections can be seen in the data from experiments with the neutrally stable beam, Fig. 7(c) red and purple lines. These imperfections are caused by the random contact between middle threaded rod and the structure of the beam. A simplified planar equivalent model was presented, based on rigid links and torsional springs, with the intention to improve the understanding of the effect of the various stiffness components within the design. This illustrative goal could be met even if this model is only of qualitative nature. It could be useful to also develop a quantitative variant of the model, where the stiffnesses of the spring relate to the dimensions of the beams, to be used as a design aid in an early design phase. This ambition is put forward as recommendation for future work.

6. Conclusion

We presented two concepts to achieve variable and switchable torsional stiffness from compliant beams using axial preload. The method shows that a variable torsional stiffness range from positive to zero and negative can be achieved by changing the preload of the high-warping-constant beam. It is also demonstrated that by applying the same preload, we can achieve zero torsional stiffness on a near-zero-warping-constant beam and that by increasing this preload, we can achieve an extending range of twisting neutral stability.

The method we used here, which is based on shortening the center axis of the beams, can be used in other ways and for other structures, e.g., wire-frame beam, to control and reduce torsional stiffness. Several techniques, such as thinning toward the center axis or varying the material stiffness toward the outside of the beam, can be used instead of transverse slits. Additionally, other methods for creating the high-warping-constant beam section, such as having curved webs, which can even lessen the stress concentration along the connection of webs and flanges, can also be used.

It is possible to use this element as a part of a larger structure that requires a repetitive simple element, e.g., origami or metamaterials, and evaluating its support stiffness as a revolute joint by changing design parameters, e.g., increasing the number of webs (m) for higher support, can be investigated in future works.

Tuning the torsional stiffness of structures and structures with zero stiffness is an important concern across several fields of research. This concept can be used in several applications where continuous rotation is not required, e.g., flexible medical devices, soft robotics, wearable robotics, legged robots, bio-mimicking robotics, and shape-morphing structures.

CRediT authorship contribution statement

Ali Amoozandeh Nobaveh: Conceptualization, Data curation, Formal analysis, Investigation, Methodology, Project administration, Software, Validation, Visualization, Writing – original draft, Writing – review & editing. **Just L. Herder:** Conceptualization, Funding acquisition, Investigation, Methodology, Project administration, Resources, Supervision, Writing – review & editing. **Giuseppe Radaelli:** Conceptualization, Formal analysis, Investigation, Methodology, Software, Supervision, Validation, Writing – original draft, Writing – review & editing.

Declaration of competing interest

The authors declare the following financial interests/personal relationships which may be considered as potential competing interests: Ali Amoozandeh Nobaveh reports financial support was provided by Dutch Research Council.

Data availability

Data will be made available on request.

Acknowledgments

This work was supported by the Dutch Research Council (NWO) [P16-05 Shell-Skeletons]. The authors would also like to thank Patrick van Holst for his assistance with the experiments.

Appendix A. Supplementary data

Supplementary material related to this article can be found online at https://doi.org/10.1016/j.mechmachtheory.2024.105607.

References

[1] L.L. Howell, Compliant mechanisms, in: 21st Century Kinematics, Springer, 2013, pp. 189–216.
[2] S.G. Nurzaman, F. Iida, L. Margheri, C. Laschi, Soft robotics on the move: scientific networks, activities, and future challenges, 2014.
[3] J. Shintake, V. Cacucciolo, D. Floreano, H. Shea, Soft robotic grippers, Adv. Mater. 30 (29) (2018) 1707035.
[4] R. Mak, A. Amoozandeh Nobaveh, G. Radaelli, J.L. Herder, A curved compliant differential mechanism with neutral stability, J. Mech. Robot. (2023) 1–11.
[5] A.A. Nobaveh, B. Caasenbrood, Design feasibility of an energy-efficient wrist flexion-extension exoskeleton using compliant beams and soft actuators, in: 2022 International Conference on Rehabilitation Robotics, ICORR, IEEE, 2022, pp. 1–6.
[6] A. Amoozandeh Nobaveh, G. Radaelli, J.L. Herder, A design tool for passive wrist support, in: Wearable Robotics: Challenges and Trends: Proceedings of the 5th International Symposium on Wearable Robotics, WeRob2020, and of WearRAcon Europe 2020, October 13–16, 2020, Springer, 2022, pp. 13–17.
[7] S. Kota, J. Joo, Z. Li, S.M. Rodgers, J. Sniegowski, Design of compliant mechanisms: applications to MEMS, Analog Integr. Circuits Signal Process. 29 (1) (2001) 7–15.
[8] K.-J. Lu, S. Kota, Design of compliant mechanisms for morphing structural shapes, J. Intell. Mater. Syst. Struct. 14 (6) (2003) 379–391.
[9] D. Li, S. Zhao, A. Da Ronch, J. Xiang, J. Drofelnik, Y. Li, L. Zhang, Y. Wu, M. Kintscher, H.P. Monner, et al., A review of modelling and analysis of morphing wings, Prog. Aerosp. Sci. 100 (2018) 46–62.
[10] D. van der Lans, A. Amoozandeh Nobaveh, G. Radaelli, Reversible shape morphing of a neutrally stable shell by untethered local activation of embedded Ni-Ti wires, J. Intell. Mater. Syst. Struct. (2023) 1045389X221151065.
[11] H. Greenberg, M. Gong, S. Magleby, L. Howell, Identifying links between origami and compliant mechanisms, Mech. Sci. 2 (2) (2011) 217–225.
[12] K. Kim, H. Heo, J. Ju, A mechanism-based architected material: A hierarchical approach to design Poisson's ratio and stiffness, Mech. Mater. 125 (2018) 14–25.
[13] A.B. Mackay, D.G. Smith, S.P. Magleby, B.D. Jensen, L.L. Howell, Metrics for evaluation and design of large-displacement linear-motion compliant mechanisms, J. Mech. Des. 134 (1) (2012).
[14] P. Wang, Q. Xu, Design and modeling of constant-force mechanisms: A survey, Mech. Mach. Theory 119 (2018) 1–21.
[15] A. Amoozandeh Nobaveh, G. Radaelli, J.L. Herder, Symmetric kinetostatic behavior from asymmetric spatially curved beams, J. Mech. Robot. 15 (4) (2023) 041010.
[16] G. Radaelli, Synthesis of Mechanisms with Prescribed Elastic Load-Displacement Characteristics (Ph.D. thesis), Delft University of Technology, Delft, The Netherlands, 2017.
[17] A. Amoozandeh Nobaveh, G. Radaelli, J.L. Herder, Asymmetric spatial beams with symmetric kinetostatic behaviour, in: ROMANSY 23-Robot Design, Dynamics and Control: Proceedings of the 23rd CISM IFToMM Symposium 23, Springer, 2021, pp. 247–254.
[18] B.D. Jensen, L.L. Howell, Bistable configurations of compliant mechanisms modeled using four links and translational joints, J. Mech. Des. 126 (4) (2004) 657–666.
[19] P.G. Opdahl, B.D. Jensen, L.L. Howell, An investigation into compliant bistable mechanisms, in: International Design Engineering Technical Conferences and Computers and Information in Engineering Conference, Vol. 80319, American Society of Mechanical Engineers, 1998, V01BT01A046.
[20] G. Radaelli, Reverse-twisting of helicoidal shells to obtain neutrally stable linkage mechanisms, Int. J. Mech. Sci. 202 (2021) 106532.
[21] D. Farhadi Machekposhti, N. Tolou, J. Herder, A review on compliant joints and rigid-body constant velocity universal joints toward the design of compliant homokinetic couplings, J. Mech. Des. 137 (3) (2015) 032301.
[22] M.R. Schultz, M.J. Hulse, P.N. Keller, D. Turse, Neutrally stable behavior in fiber-reinforced composite tape springs, Composites A 39 (6) (2008) 1012–1017.
[23] J.P. Stacey, M.P. O'Donnell, M. Schenk, Thermal prestress in composite compliant shell mechanisms, J. Mech. Robot. 11 (2) (2019) 020908.
[24] T. Murphey, S. Pellegrino, A novel actuated composite tape-spring for deployable structures, in: 45th AIAA/ASME/ASCE/AHS/ASC Structures, Structural Dynamics & Materials Conference, 2004, p. 1528.
[25] C. Vehar, S. Kota, R. Dennis, Closed-loop tape springs as fully compliant mechanisms: preliminary investigations, in: International Design Engineering Technical Conferences and Computers and Information in Engineering Conference, Vol. 46954, 2004, pp. 1023–1032.
[26] S. Guest, E. Kebadze, S. Pellegrino, A zero-stiffness elastic shell structure, J. Mech. Mater. Struct. 6 (1) (2011) 203–212.
[27] E. Lamacchia, A. Pirrera, I. Chenchiah, P. Weaver, Non-axisymmetric bending of thin annular plates due to circumferentially distributed moments, Int. J. Solids Struct. 51 (3–4) (2014) 622–632.
[28] K. Seffen, R. McMahon, Heating of a uniform wafer disk, Int. J. Mech. Sci. 49 (2) (2007) 230–238.
[29] S. Kok, G. Radaelli, A.A. Nobaveh, J. Herder, Neutrally stable transition of a curved-crease planar shell structure, Extreme Mech. Lett. 49 (2021) 101469.
[30] S. Kok, A.A. Nobaveh, G. Radaelli, Neutrally stable double-curved shells by inflection point propagation, J. Mech. Phys. Solids (2022) 105133.
[31] N. Tolou, V.A. Henneken, J.L. Herder, Statically balanced compliant micro mechanisms (SB-MEMS): Concepts and simulation, in: International Design Engineering Technical Conferences and Computers and Information in Engineering Conference, Vol. 44106, 2010, pp. 447–454.
[32] N. Tolou, J.L. Herder, Concept and modeling of a statically balanced compliant laparoscopic grasper, in: International Design Engineering Technical Conferences and Computers and Information in Engineering Conference, Vol. 49040, 2009, pp. 163–170.
[33] K. Hoetmer, G. Woo, C. Kim, J. Herder, Negative stiffness building blocks for statically balanced compliant mechanisms: Design and testing, J. Mech. Robot. 2 (4) (2010).
[34] R. Mak, A. Amoozandeh Nobaveh, G. Radaelli, J.L. Herder, A curved compliant differential mechanism with neutral stability, in: International Design Engineering Technical Conferences and Computers and Information in Engineering Conference, Vol. 86281, American Society of Mechanical Engineers, 2022, V007T07A004.
[35] S. Yuan, Y. Sun, M. Wang, J. Ding, J. Zhao, Y. Huang, Y. Peng, S. Xie, J. Luo, H. Pu, et al., Tunable negative stiffness spring using maxwell normal stress, Int. J. Mech. Sci. 193 (2021) 106127.
[36] I.K. Kuder, A.F. Arrieta, W.E. Raither, P. Ermanni, Variable stiffness material and structural concepts for morphing applications, Prog. Aerosp. Sci. 63 (2013) 33–55.
[37] J. Sun, Q. Guan, Y. Liu, J. Leng, Morphing aircraft based on smart materials and structures: A state-of-the-art review, J. Intell. Mater. Syst. Struct. 27 (17) (2016) 2289–2312.
[38] H. Akhavan, P. Ribeiro, M. De Moura, Large deflection and stresses in variable stiffness composite laminates with curvilinear fibres, Int. J. Mech. Sci. 73 (2013) 14–26.
[39] L. Blanc, A. Delchambre, P. Lambert, Flexible medical devices: Review of controllable stiffness solutions, in: Actuators, Vol. 6, Multidisciplinary Digital Publishing Institute, 2017, p. 23.
[40] H.M. Le, L. Cao, T.N. Do, S.J. Phee, Design and modelling of a variable stiffness manipulator for surgical robots, Mechatronics 53 (2018) 109–123.
[41] A. Dunning, J. Stroo, G. Radaelli, J. Herder, Feasibility study of an upper arm support based on bending beams, in: 2015 IEEE International Conference on Rehabilitation Robotics, ICORR, IEEE, 2015, pp. 520–525.
[42] S. Jadhav, M.R.A. Majit, B. Shih, J.P. Schulze, M.T. Tolley, Variable stiffness devices using fiber jamming for application in soft robotics and wearable haptics, Soft Robot. 9 (1) (2022) 173–186.
[43] A.A. Nobaveh, G. Radaelli, W.W. van de Sande, R.A. van Ostayen, J.L. Herder, Characterization of spatially curved beams with anisotropically adaptive stiffness using sliding torsional stiffeners, Int. J. Mech. Sci. 234 (2022) 107687.

[44] T. Jin, Z. Liu, S. Sun, Z. Ren, L. Deng, D. Ning, H. Du, W. Li, Theoretical and experimental investigation of a stiffness-controllable suspension for railway vehicles to avoid resonance, Int. J. Mech. Sci. 187 (2020) 105901.
[45] H. Zhao, C. Zhao, S. Ren, S. Bi, Analysis and evaluation of a near-zero stiffness rotational flexural pivot, Mech. Mach. Theory 135 (2019) 115–129, http://dx.doi.org/10.1016/j.mechmachtheory.2019.02.003, URL https://www.sciencedirect.com/science/article/pii/S0094114X19300941.
[46] M. Smreczak, L. Tissot-Daguette, E. Thalmann, C. Baur, S. Henein, A load cell with adjustable stiffness and zero offset tuning dedicated to electrical micro- and nanoprobing, Precis. Eng. 76 (2022) 208–225, http://dx.doi.org/10.1016/j.precisioneng.2022.03.009, URL https://www.sciencedirect.com/science/article/pii/S014163592200068X.
[47] P. Bilancia, S.P. Smith, G. Berselli, S.P. Magleby, L.L. Howell, Zero torque compliant mechanisms employing pre-buckled beams, J. Mech. Des. 142 (11) (2020) 113301.
[48] J. Li, K. Fu, Y. Gu, Z. Zhao, Torsional negative stiffness mechanism by thin strips, Theor. Appl. Mech. Lett. 9 (3) (2019) 206–211.
[49] M.R. Schultz, A concept for airfoil-like active bistable twisting structures, J. Intell. Mater. Syst. Struct. 19 (2) (2008) 157–169.
[50] K.A. Seffen, S.D. Guest, Prestressed morphing bistable and neutrally stable shells, J. Appl. Mech. 78 (1) (2011).
[51] X. Lachenal, S. Daynes, P.M. Weaver, A non-linear stiffness composite twisting I-beam, J. Intell. Mater. Syst. Struct. 25 (6) (2014) 744–754.
[52] A.A. Nobaveh, J.L. Herder, G. Radaelli, A compliant Continuously Variable Transmission (CVT), Mech. Mach. Theory 184 (2023) 105281.